Supporting Information

Unraveling the Sorption Mechanism of Industrial Dyes onto Zr-based MOF: a Computational and Experimental Modelling for Highly Efficient Removal

Kora Lucresse Tiomo Nguena[1,2], Cyrille Ghislain Fotsop[1,3], Aurelien Bopda[1], Donald Raoul Tchuifon Tchuifon[1,4], Fredy Harcel Kamgang Djioko[2,5], Alvine Mirabelle Soukoua Ngueabouo[1,], Chinyere Ada Madu[2], Fabian I. Ezema[2,6], Emeka Emmanuel Oguzie[2]

Table S1 : Central composite design for the adsorption of indigo carmine, rhodamin B and orange 2.

N°	Time (min)	Concentration (mg/L)	pH	Masse (mg)
1.	30	20	2	20
2.	120	20	2	20
3.	30	200	2	20
4.	120	200	2	20
5.	30	20	10	20
6.	120	20	10	20
7.	30	200	10	20
8.	120	200	10	20
9.	30	20	2	80
10.	120	20	2	80
11.	30	200	2	80
12.	120	200	2	80
13.	30	20	10	80
14.	120	20	10	80
15.	30	200	10	80
16.	120	200	10	80
17.	30	110	6	50
18.	120	110	6	50
19.	75	20	6	50
20.	75	200	6	50
21.	75	110	2	50
22.	75	110	10	50
23.	75	110	6	20
24.	75	110	6	80
25.	75	110	6	50
26.	75	110	6	50
27.	75	110	6	50
28.	75	110	6	50

Table S2: Kinetic models in nonlinear forms

Kinetic models	Non-linear forms	Reference
Pseudo-first order	$Q_t = Q_e[1 - exp(-K_1 t)]$	1

Pseudo-second order	$Q_t = \frac{Q_e^2 K_2 t}{1 + Q_e K_e t}$	1
Elovich model	$Q_t = \frac{ln(\alpha\beta)}{\beta} + \frac{ln\, t}{\beta}$	1
Intraparticle diffusion	$Q_t = K_{\text{int}} t^{\frac{1}{2}} + C$	1

Table S3: Non-linear isotherms models forms

Parameters	Isotherms	Non-linear forms	References
Two	**Langmuir**	$Q_e = \frac{Q_m K_L C_e}{1 + K_L C_e}$	2
	Freundlich	$Q_e = K_F Ce^{\frac{1}{n}}$	2
Three	**Toth**	$Q_e = \frac{Q_m K_T C_e}{[1 + (K_T C_e)^n]^{1/n}}$	3

Langmuir separation factor (R_L) : $R_L = \frac{1}{1 + K_L C_O}$ Eq.S1 [4]

Table S4: Equations for error functions

Error function	Abbreviation	formula	References
Coefficient of determination	R^2	$\frac{\sum_{i=1}^{N}(Q_{e,cal} - Q_{m\exp})^2}{\sum_{i=1}^{N}(Q_{e,cal} - Q_{m\exp})^2 + (Q_{e,cal} - Q_{m\exp})^2}$	3
Residual Root Mean Square Error	RMSE	$\sqrt{\frac{1}{n-2}\sum_{i=1}^{N}(Q_{e,\exp} - Q_{e,cal})^2}$	5
Chi-square test	χ^2	$\sum_{i=1}^{N}\frac{(Q_{e,\exp} - Q_{e,cal})^2}{Q_{e,cal}}$	5
Hybrid Fractional Error Function	HYBRID	$\frac{100}{N-p}\sum_{i=1}^{N}\left[\frac{(Q_{e,i,\exp} - Q_{e,i,cal})^2}{Q_{e,i,\exp}}\right]$	3
Average Relative Error	ARE	$\frac{100}{N}\sum_{i=1}^{N}\left\lvert\frac{Q_{e,i,cal} - Q_{e,i,\exp}}{Q_{e,i,\exp}}\right\rvert$	3

Where N is the number of experimental data points, Qe_{cal} (mg/g) is the theoretically calculated adsorption capacity at equilibrium, Qe_{exp} (mg/g) is the experimental adsorption capacity at equilibrium, p denotes the number of parameter

$\Delta Egap = E_{LUMO} - E_{HOMO}$ Eq.S2 [6]

Table S5: Summary of N_2 adsorption-desorption analyses of NH_2-UiO-66

Samples	BET surface ($m^2.g^{-1}$)	Total pore volume ($cm^3.g^{-1}$)	External surface area ($m^2.g^{-1}$)	Micropore area ($m^2.g^{-1}$)	Micropore volume ($cm^3.g^{-1}$)
NH_2-UiO-66	1156.62	0.66884	305.58	851.03	0.440253

Table S6: Central composite design for the adsorption (residual) of Indigo carmine, Rhodamin B and Orange 2.

N°	Time (min)	Concentration (mg/L)	pH	Masse (mg)	Y1: Adsorption of Indigo carmine (mg/g)	Y2: Adsorption of Rhodamin B (mg/g)	Y3: Adsorption of Orange II (mg/g)
					Residual	Residual	Residual
1.	-1	-1	-1	-1	1.94	0.83	11.7
2.	+1	-1	-1	-1	-1.1	0.84	-2.05
3.	-1	+1	-1	-1	1.33	3.07	-10.9
4.	+1	+1	-1	-1	0.43	-6.24	3.96
5.	-1	-1	+1	-1	-7.66	-1.79	1.21
6.	+1	-1	+1	-1	6.32	1.17	-11.36
7.	-1	+1	+1	-1	-2.1	0.77	9.94
8.	+1	+1	+1	-1	9.51	-0.35	16
9.	-1	-1	-1	+1	-11.68	-2.32	-15.353
10.	+1	-1	-1	+1	3.2	1.61	-6.67
11.	-1	+1	-1	+1	-5.22	1.21	14.62
12.	+1	+1	-1	+1	5.49	-0.88	-0.56
13.	-1	-1	+1	+1	0.67	8.62	-0.69
14.	+1	-1	+1	+1	-3.5	-5.74	11.55
15.	-1	+1	+1	+1	-1.07	-3.51	2.71
16.	+1	+1	+1	+1	-0.83	1.55	-8.44
17.	-1	0	0	0	23.79	-6.88	-13.24
18.	+1	0	0	0	-19.52	8.04	-2.43
19.	0	-1	0	0	11.81	-3.22	11.67
20.	0	+1	0	0	-7.55	4.38	-27.34
21.	0	0	-1	0	5.6	1.87	5.25
22.	0	0	+1	0	-1.33	-0.71	-20.92
23.	0	0	0	-1	-8.67	1.71	-18.5
24.	0	0	0	+1	12.94	-0.55	2.84
25.	0	0	0	0	11.93	-0.92	9.83
26.	0	0	0	0	-28.25	-0.97	8.42
27.	0	0	0	0	-8.29	-0.94	9.36
28.	0	0	0	0	11.8	-0.64	19.4

Residual = Predicted value - Observed values

Table S7: Optimal conditions for the adsorption and predicted and experimental values.

	Conditions			Adsorption (mg/g)		
	Concentration	pH	Mass	Predicted	Experimental	Error

Responses	Time (min)	(g/mL)	(%)	(mg)	value	value	percentage
Indigo Carmine	60	100	10	22	265.48	264.81	0.67
Rhodamin B	120	90	5.28	26	95.98	91.62	4.35
Orange 2	88.90	100	7.16	23	230.67	229.89	0.78

Table S8: Parameters of the isotherm models for adsorption of dyes

Dyes	Isotherm	Parameters	REQM	HYBRID	SEA	ERM	R^2	χ
IC	Langmuir	K_L = 0.04071 q_{mL}= 433640.982 R_L = 0.19719	17.732	17.732	5.069	0.108	0.510	1.350
	Freundlich	K_F= 6.627 n_F =0.708	17.689	33.597	1.377	0.036	0.766	1.343
	Toth	q_{mT}= 17.229 a_T = 147.494 n_T = 0.0001	4.990	10.493	2.970	0.178	0.982	0.629
O2	Langmuir	K_L = 0.092 q_{mL}= 558.919 R_L = 0.09803	16.901	31.941	37.419	0.836	0.977	1.217
	Freundlich	K_F= 6.919 n_F =0.092	16.901	31.941	37.419	0.836	0.826	1.077
	Toth	q_{mT}= 135.688 a_T = 0.106 n_T = 2.880	3.472	5.392	-4.916	-0.314	0.991	0.323
RhB	Langmuir	K_L = 0.00425 q_{mL}=1417330.000 R_L = 0.723327	7.093	35.733	7.921	1.125	0.894	1.429
	Freundlich	K_F= 0.055 n_F = 0.761	6.437	29.435	2.273	0.403	0.722	1.177
	Toth	q_{mT}= 33.437 a_T = 93.204 n_T = 0.0001	0.259	0.971	0.299	0.614	0.852	0.058

Table S9: Parameters of the kinetic models for adsorption of dyes

Dyes	Kinetic	Parameters	REQM	HYBRID	SEA	ERM	R^2	χ^2
IC	Pseudo-first order	Qe = 93.795 K= 0.0602	11.1194	18.6205	-67.7395	-1.0202	0.9827	1.4896
	Pseudo-second order	Qe =106.4678 K=7.48E-04	4.1589	1.7366	3.5674	0.0358	0.9976	0.1607
	Elovich	α=22.0978 B=0.0493	4.2617	2.1882	-9.3670	-0.1026	0.9975	0.1969
	Intraparticular diffusion	Kp=7.5716 C=21.8299	10.4022	13.0366	-0.0003	-3.02E-06	0.9824	1.4340
O2	Pseudo-first order	Qe=91.8919 K= 0.1338	2.8136	1.0742	-2.0685	-0.0281	0.9990	0.0859
	Pseudo-second order	Qe =98.4952 K=0.0023	2.0103	0.3656	-0.1717	-0.0016	0.9995	0.0439
	Elovich	α=393.1846 B=0.0848	5.8570	3.7242	-0.1201	-0.0012	0.9961	0.3352
	Intraparticular	Kp=5.9323	16.7199	30.3495	-5.533E-	-5.46E-	0.9594	3.3384

	diffusion	C=39.6709			05	07		
RhB	Pseudo-first order	Qe=15.6020 K=0.1189	1.5755	2.0085	-0.8326	-0.067	0.9896	0.1607
	Pseudo-second order	Qe =17.1640 K=0.0099	0.9912	0.5299	0.2474	0.0133	0.9959	0.0636
	Elovich	α=17.8994 B=0.3958	0.6118	0.2423	-0.1857	-0.0109	0.9985	0.0218
	Intraparticle diffusion	Kp=1.1682 C=5.5708	2.1926	3.1120	4.98E-06	2.93E-07	0.9761	0.3423

Table S10: Thermodynamiques parameters

Dyes	ΔH°(kJ/mol)	ΔS°(J/mol.K)	ΔG° (kJ/mol)		
			298 K	308 K	318 K
IC	-81.18	-243.22	-8.70	-6.27	-3.83
RhB	-17.05	-70.08	3.82	4.53	5.23
O2	-64.60	-196.05	-6.19	-4.23	-2.27

Table S11: Comparison of adsorption capacities of different dyes

Adsorbent	Adsorbate	Capacity/(mg/g)	Ref
α-Fe2O3/NiS	Alizarin R S	91	[7]
activated carbon doped with Mn oxide (Bio-MnO_x-C)	Indigo carmine	45.95	[7]
NH_2-UiO-66	Methylene Blue	97.97	[8]
	Rhodamine B	82.69	
	Safranin dye	390	[9]
UiO-66	Methylene Blue	90.59	[8]
	Rhodamine B	77.47	
	Methylene Blue	83.9	[7]
	Methyl Orange	175.4	
	Rhodamine	75.85	[10]
	Indigo carmine	75.89	[11]
UiO-66-0.5ATA	Indigo carmine	69.55	[11]
UiO-66-0.75ATA	Indigo carmine	84.26	[11]
UiO-66-ATA	Indigo carmine	66.67	[11]
NH_2-UiO-66	Indigo carmine	265.8	Present study
NH_2-UiO-66	Orange 2	229.8	Present study
NH_2-UiO-66	Rhodamine B	91.6	Present study

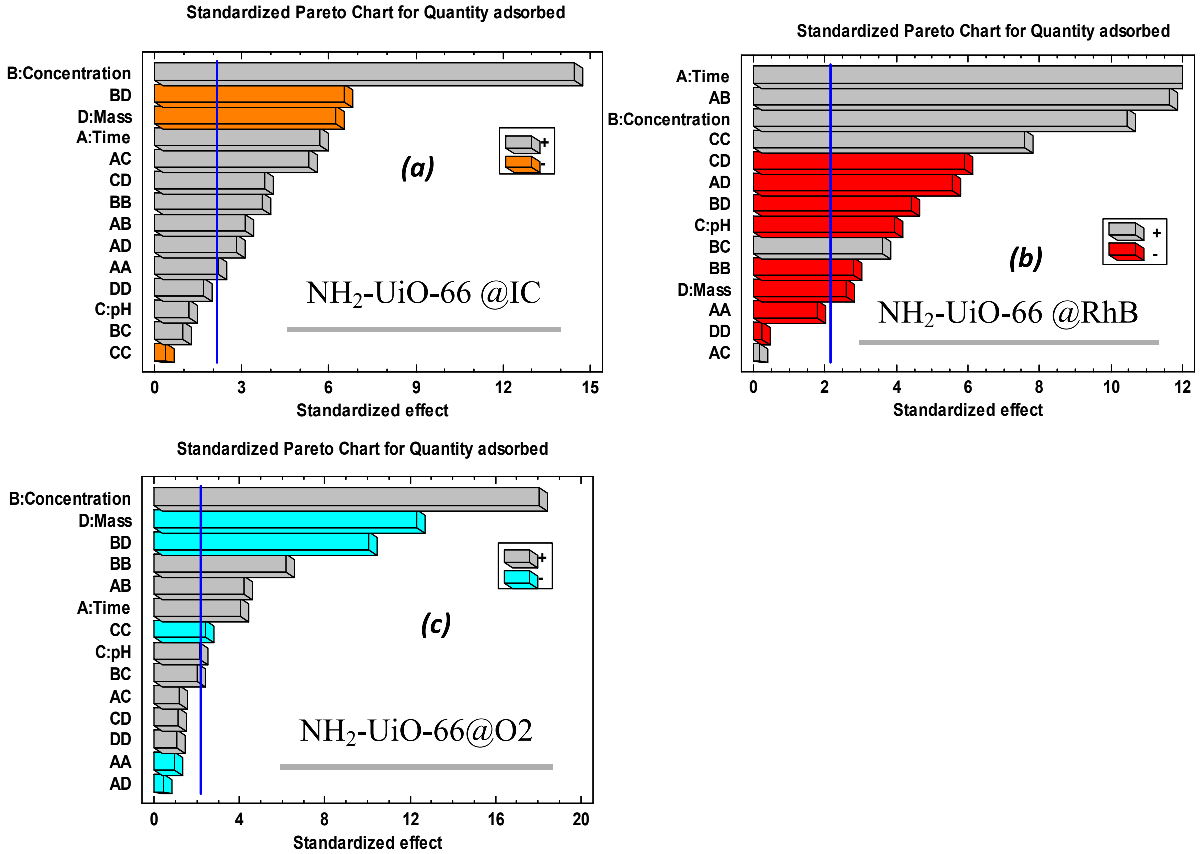

Fig. S1. Pareto diagrams of the effects of factors A, B, C and D for organic dyes IC (a), RhB (b) and O2 (c) adsorption

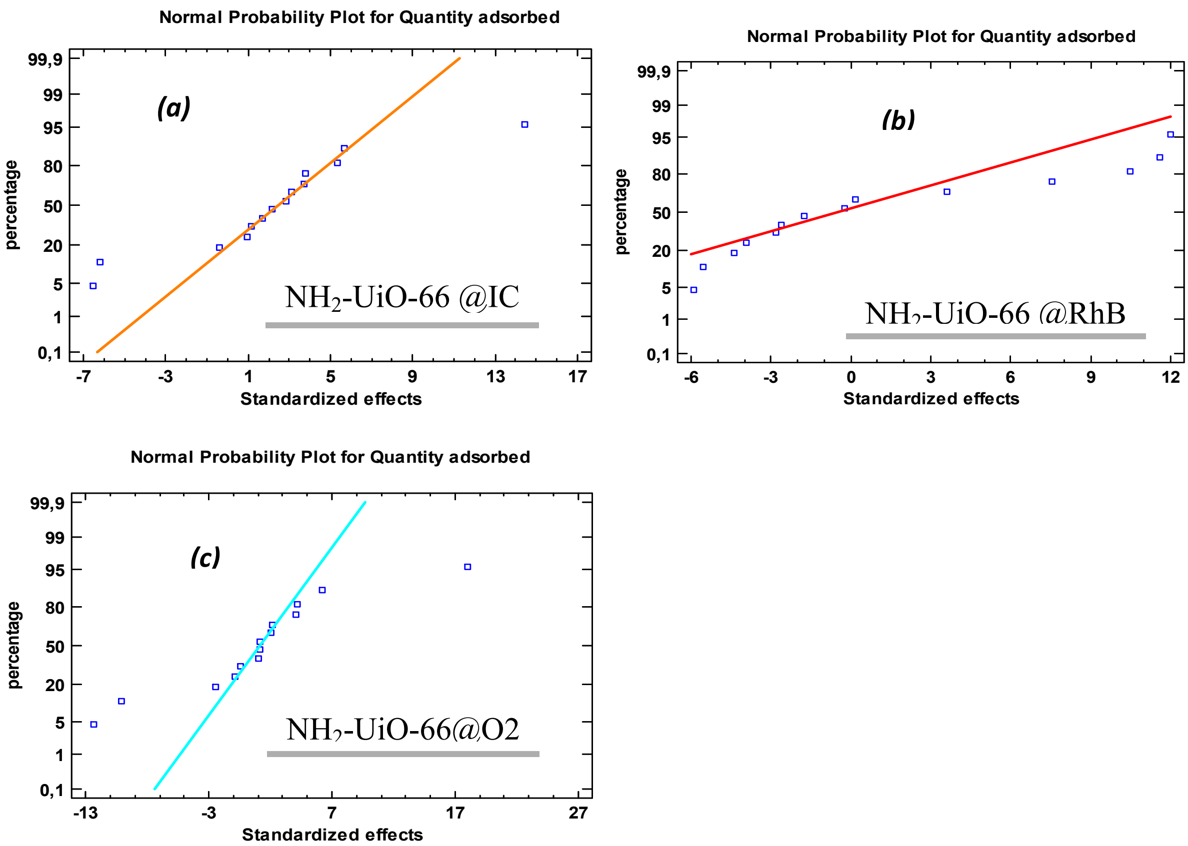

Fig. S2. Normal probability plot for the quantity of IC (a), RhB (b) and O2 (c) adsorbed

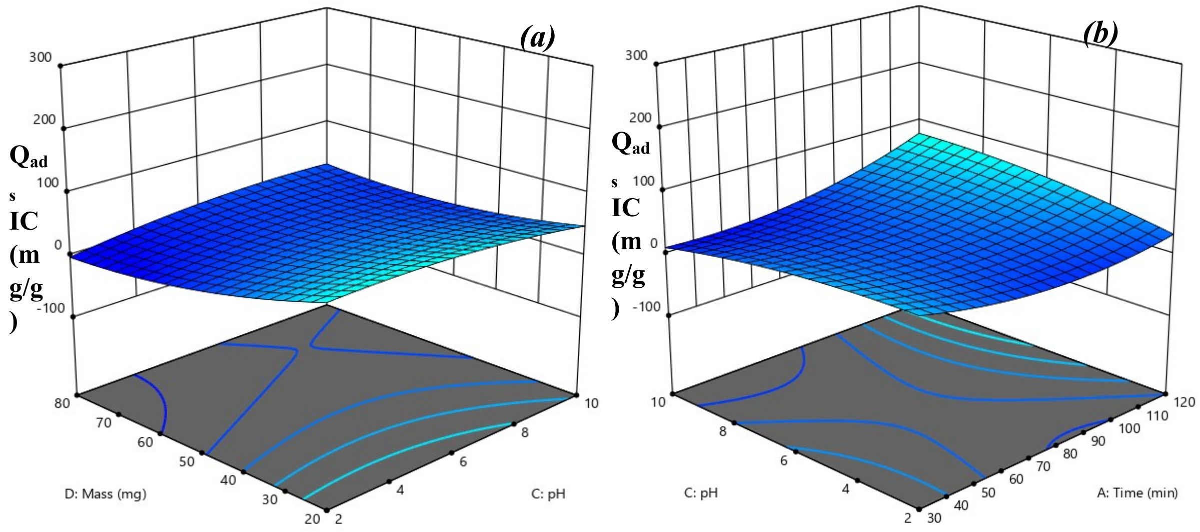

Fig. S3. Response surface plots of the central composite design showing the effect of time (min), pH and mass (mg) on the adsorption of the indigo carmine (mg/g)

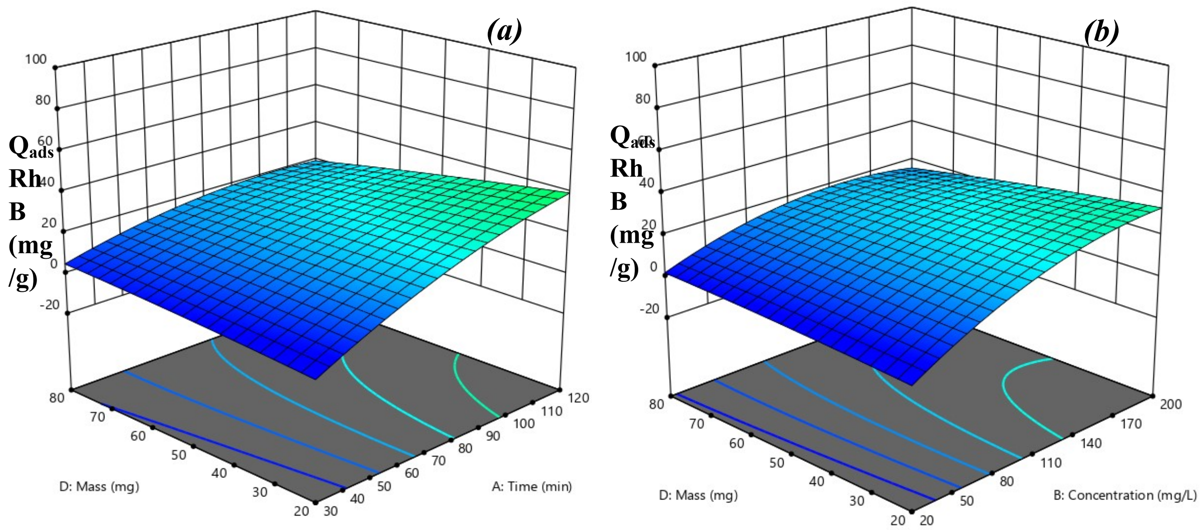

Fig. S4. Response surface plots of the central composite design showing the effect of time (min), concentration (mg/L) and mass (mg) on the adsorption of the rhodamin B (mg/g)

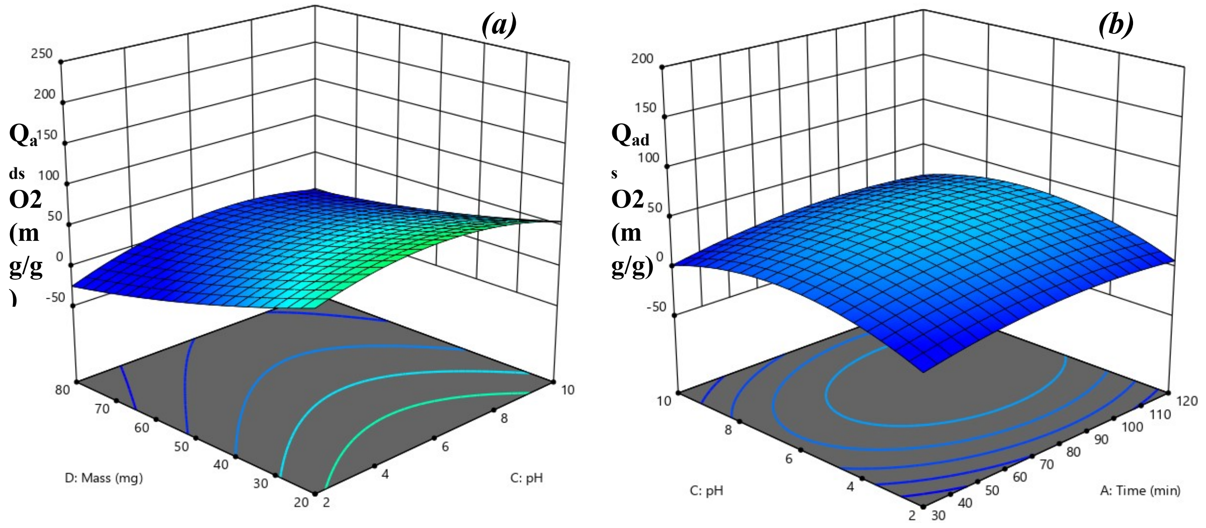

Fig. S5. Response surface plots of the central composite design showing the effect of time (min), pH and mass (mg) on the adsorption of the orange 2 (mg/g).

Isotherm

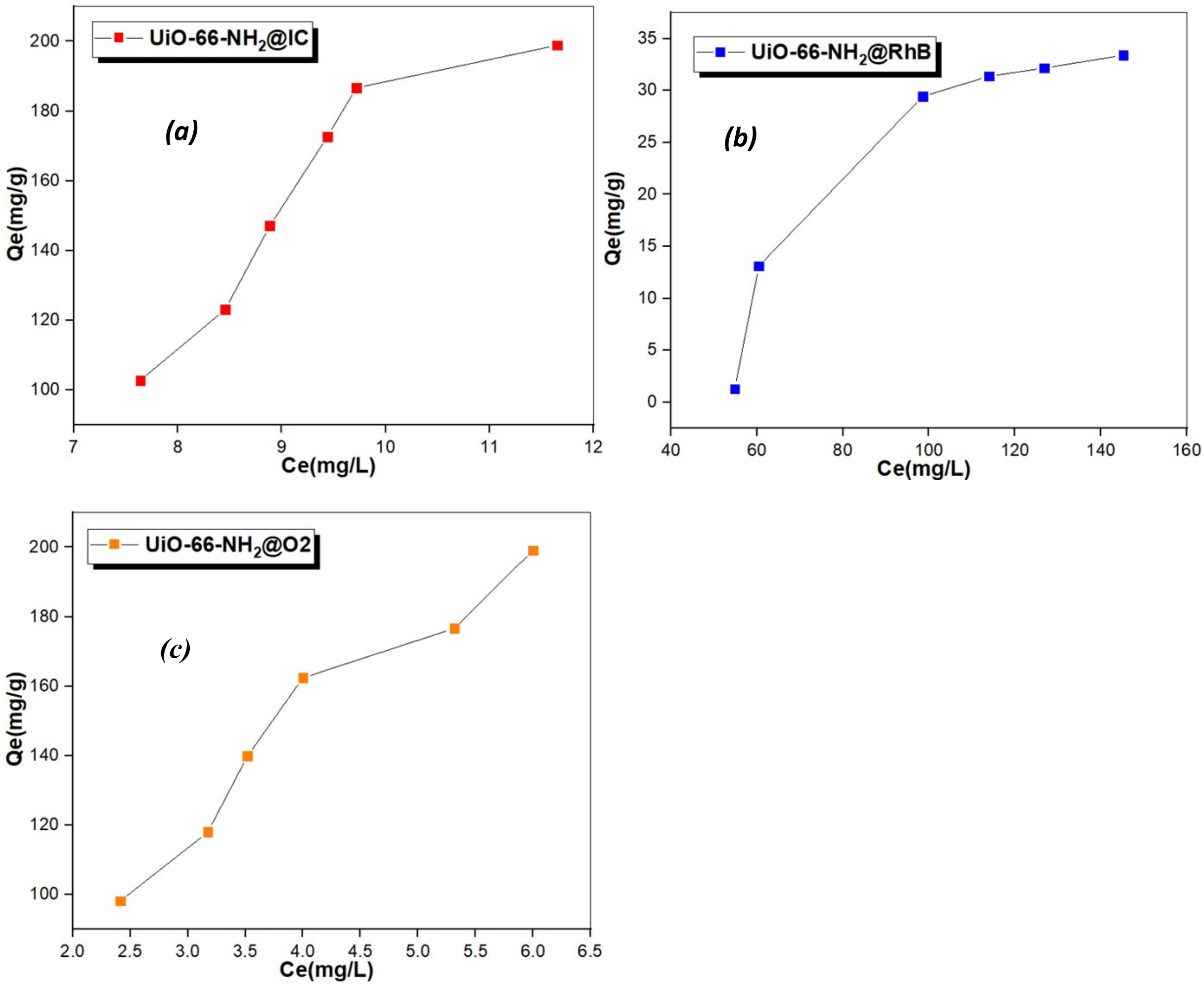

Fig. S6. Impact of concentration on the adsorption of indigo carmine (a), rhodamine B (b) and orange 2 (c) using NH_2-UiO-66

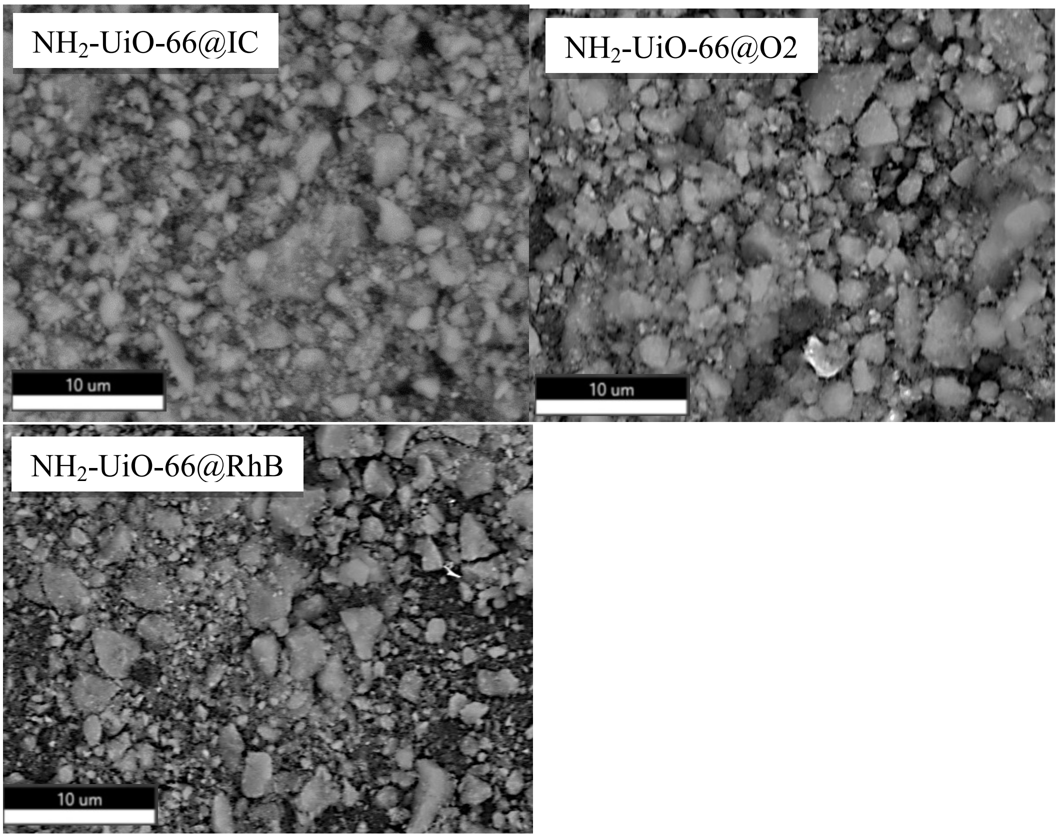

Fig. S7. SEM images of NH_2-UiO-66 after indigo carmine (IC) (a), rhodamine B (RhB) (b) and orange 2 (O2) (c) adsorption

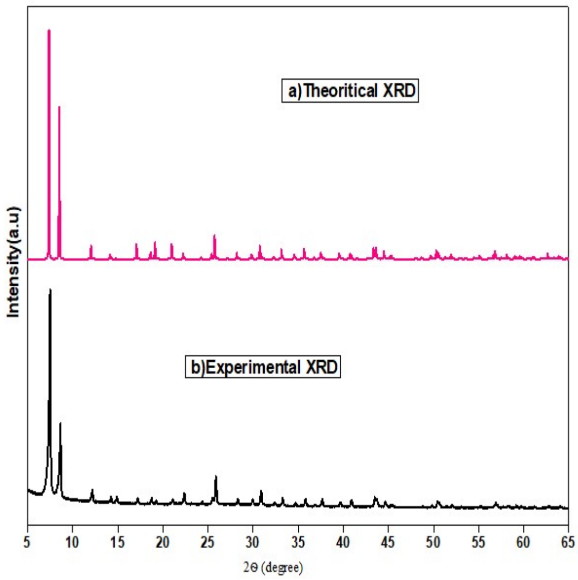

Fig. S8. Experimental and theoretical XRD pattern of NH_2-UiO-66

Molecular dynamic simulation

Total, adsorption and interaction energies were evaluated as follows [12]**:**

$$E_{Interaction} = E_{Tot} - (E_{Surface} + E_{Polluant}) \quad \text{Eq.S3}$$

Among them, E_{Tot} represents the total adsorption energy of the studied species on the NH_2-UiO-66 surface, and $E_{surface}$ and $E_{pollutant}$ are respectively the total energy of clean NH_2-UiO-66 plate and isolated molecules. The binding energy is the absolute value of the interaction energy.

$$E_{Liaison} = - E_{Iinteraction} \qquad \text{Eq.S4}$$

Table S12: Energies E_{HOMO}, E_{LUMO} and Egap of IC, RhB and O2 studied

Energies (eV)	IC	O2	RhB
E_{HOMO}	-0.197	-0.217	- 0.177
E_{LUMO}	-0.154	-0.134	-0.122
ΔEgap	0.043	0.086	0.055
ΔN	4.119	2.097	2.707

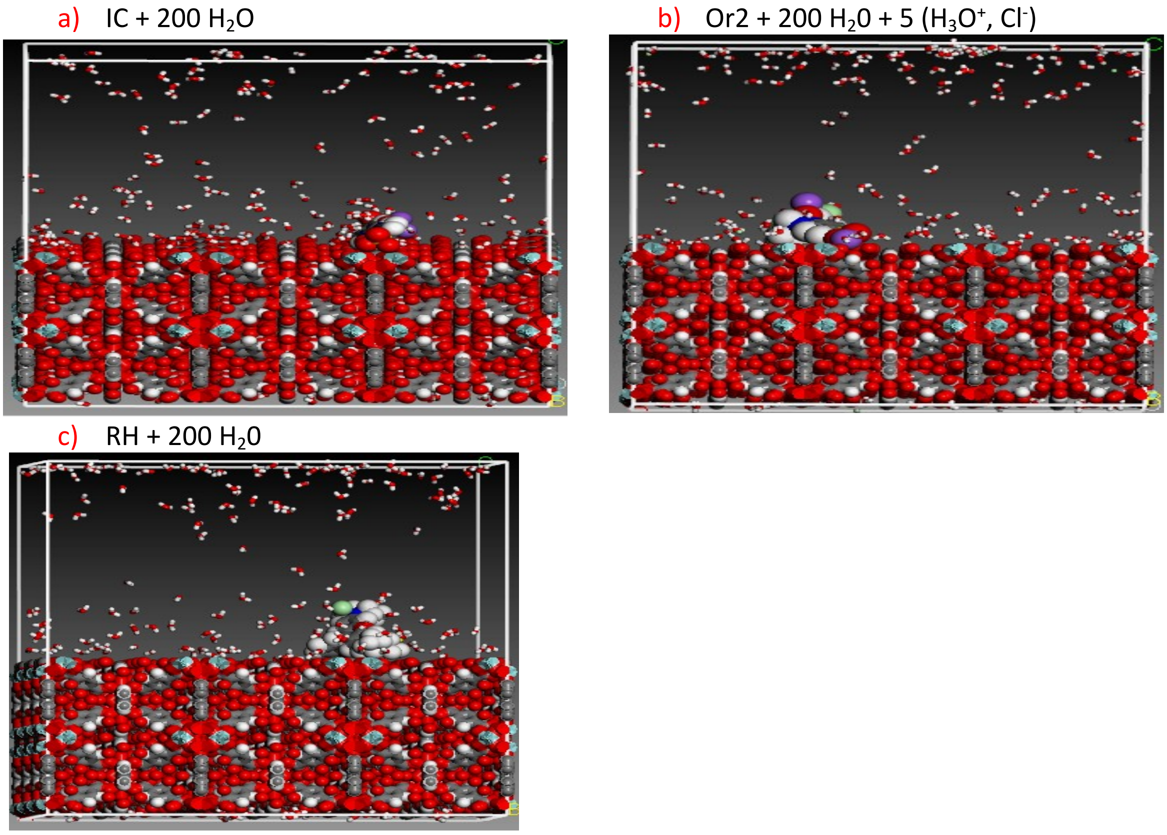

Fig. S9. Front views of the most stable low-energy configuration for adsorption of IC, O2 and RhB molecules on the NH2-UiO-66 surface at 298 K.

Reference

1. Mokue Mafo, S. G. *et al.* Low-cost magnetic carbons-based rubber seed husks materials for highly efficient removal for reactive black 5 and reactive blue 19 textile dyes from wastewater. *Int. J. Environ. Anal. Chem.* 1–25 (2023) doi:10.1080/03067319.2023.2269857.
2. Atemkeng, C. D. *et al.* Optimization of 4-nonylphenol adsorption on activated carbons derived from safou seeds using response surface methodology. *Carbon Trends* **4**, 100052 (2021).
3. Nguena, K. L. T. *et al.* Mathematical modeling approach for the green synthesis of high-performance nanoporous zeolites Na-X optimized for water vapor sorption. *Mater. Today Commun.* **37**, 107406 (2023).

4. Kamgang Djioko, F. H. *et al.* Efficient removal of pharmaceutical contaminant in wastewater using low-cost zeolite 4A derived from kaolin: Experimental and theoretical studies. *Mater. Chem. Phys.* **315**, 128994 (2024).
5. Zemfack Mekuiko, A. *et al.* Tailoring activated carbons based cocoa pods lignocellulosic materials for Reactive blue 19 adsorption: optimization, adsorption isotherm and kinetic investigation. *DESALINATION WATER Treat.* **300**, 144–157 (2023).
6. Tiomo, L. K. N., Madu, C. A., Ezema, F. I., Ngoune, J. & Oguzie, E. E. Molecular modelling of energy storage performance on metal organic frameworks/ethane nanoparticles nanofluids mixtures and derivatives. *Mater. Today Commun.* **38**, 107756 (2024).
7. Embaby, M. S., Elwany, S. D., Setyaningsih, W. & Saber, M. R. The adsorptive properties of UiO-66 towards organic dyes: A record adsorption capacity for the anionic dye Alizarin Red S. *Chin. J. Chem. Eng.* **26**, 731–739 (2018).
8. Chen, Q. *et al.* Selective adsorption of cationic dyes by UiO-66-NH2. *Appl. Surf. Sci.* **327**, 77–85 (2015).
9. Tambat, S. N. *et al.* Hydrothermal synthesis of NH2-UiO-66 and its application for adsorptive removal of dye. *Adv. Powder Technol.* **29**, 2626–2632 (2018).
10. He, Q., Chen, Q., Lü, M. & Liu, X. Adsorption Behavior of Rhodamine B on UiO-66. *Chin. J. Chem. Eng.* **22**, 1285–1290 (2014).
11. Nanthamathee, C., Chantarangkul, C., Jakkrawhad, C., Payaka, A. & Dechatiwongse, P. Fine-Tuning Dye Adsorption Capacity of UiO-66 by Mixed-Ligand Approach. Preprint at https://doi.org/10.21203/rs.3.rs-490186/v1 (2021).
12. Njoku, D. I., Li, Y., Lgaz, H. & Oguzie, E. E. PT NU SC. *J. Mol. Liq.* (2017) doi:10.1016/j.molliq.2017.11.051.